

## Article

# Recognition of Heavy Metals by Using Resorcin[4]arenes Soluble in Water

Edilma Sanabria <sup>1</sup>, Miguel A. Esteso <sup>2,3,\*</sup> and Edgar F. Vargas <sup>4,\*</sup>

<sup>1</sup> Grupo GICRIM, Programa de Investigación Criminal, Universidad Manuela Beltrán, Avenida Circunvalar No. 60-00, Bogotá 111321, Colombia

<sup>2</sup> Universidad Católica de Ávila, Calle los Canteros s/n, 05005 Ávila, Spain

<sup>3</sup> Unidad Docente Química Física, Universidad de Alcalá, 28805 Alcalá de Henares (Madrid), Spain

<sup>4</sup> Departamento de Química, Universidad de los Andes, Cr. 1 No. 18A 10, Bogotá 111711, Colombia

\* Correspondence: [mangel.esteso@ucavila.es](mailto:mangel.esteso@ucavila.es) (M.A.E.); [edvargas@uniandes.edu.co](mailto:edvargas@uniandes.edu.co) (E.F.V.)

**Abstract:** The complexing properties of two water-soluble resorcin[4]arenes (tetrasodium 5,11,17,23-tetrakisulfonatemethylen-2,8,14,20-tetra(butyl)resorcin[4]arene, Na<sub>4</sub>BRA, and tetrasodium 5,11,17,23-tetrakisulfonatemethylen-2,8,14,20-tetra(2-(methylthio)ethyl)resorcin[4]arene, Na<sub>4</sub>SRA) with polluting heavy metals such as Cu<sup>2+</sup>, Pb<sup>2+</sup>, Cd<sup>2+</sup> and Hg<sup>2+</sup> were studied by conductivity, and the findings were confirmed by using other techniques to try to apply this knowledge to removing them. The results indicate that Na<sub>4</sub>BRA is able to complex Cu<sup>2+</sup> in a 1:1 ratio and Pb<sup>2+</sup> in a 1:2 ratio, while Na<sub>4</sub>SRA complexes Hg<sup>2+</sup> in a 1:1 ratio. On the contrary, no indications have been observed that either of the resorcin[4]arenes studied complexes the Cd<sup>2+</sup> ions. The results suggest that the bonds established between the sulfur atoms located at the lower edge of the SRA<sup>4-</sup> and the solvent hydrogens could prevent the entry of the guest into the host cavity. However, in the case of Hg<sup>2+</sup> ions, the entry is favoured by the interactions between the sulfur donor atoms present on the lower edge of Na<sub>4</sub>SRA and the Hg<sup>2+</sup> ions. Therefore, it can be said that Na<sub>4</sub>BRA is selective for Cu<sup>2+</sup> and Pb<sup>2+</sup> ions and Na<sub>4</sub>SRA is selective for Hg<sup>2+</sup> ions.



**Citation:** Sanabria, E.; Esteso, M.A.; Vargas, E.F. Recognition of Heavy Metals by Using Resorcin[4]arenes Soluble in Water. *Toxics* **2022**, *10*, 461. <https://doi.org/10.3390/toxics10080461>

Academic Editor: Tiziana Missana and Fuli Xu

Received: 11 May 2022

Accepted: 1 August 2022

Published: 9 August 2022

**Publisher's Note:** MDPI stays neutral with regard to jurisdictional claims in published maps and institutional affiliations.



**Copyright:** © 2022 by the authors. Licensee MDPI, Basel, Switzerland. This article is an open access article distributed under the terms and conditions of the Creative Commons Attribution (CC BY) license (<https://creativecommons.org/licenses/by/4.0/>).

**Keywords:** heavy metals; inorganic pollutants; resorcin[4]arenes; recognition

## 1. Introduction

Soil contamination by heavy metals poses a great risk to human health, animals, plants, microorganisms and their interactions [1]. In humans, for example, prolonged exposure to contaminated soils has negative effects on the central nervous system, the gastric system and the respiratory system [2,3]. Additionally, heavy metals can cause great ecological risk when they are absorbed by different aquatic organisms, thus entering the food chain [4]. They also affect the functioning of soil enzymes and microbial biomass (affecting microorganisms is crucial since they play an important role in the cycle of nutrients and in the decomposition of matter), hindering their growth and consequently degrading the quality of the soil. Examples of the above are those produced by Pb, which has effects on bacteria, and by Cd, which impacts the fungal population [5]. The fate and effect of these pollutants depend on the geographical and environmental conditions, the nature of the soil and the type of human activities, including the use of agrochemicals [6,7], mining [8–11] and industrial activities [12,13].

Aware of the problem, this research seeks to show progress in the recognition of certain polluting heavy metals in solution, such as Cu<sup>2+</sup>, Pb<sup>2+</sup>, Cd<sup>2+</sup> and Hg<sup>2+</sup>, using complexing macrocycles such as the resorcin[4]arenes, to try to apply it in their removal. Although, when Cu is present in the human body in amounts that do not exceed 75–100 mg, it is vital for health, when the concentration of this metal is higher, various disorders occur such as nausea, vomiting, abdominal pain and cramps, headache, dizziness, weakness and diarrhea, among others; such disorders occur mainly in the case of individuals with liver

diseases and other pathologies in which the excretion of bile is compromised [14]. The effect of lead (Pb) on humans is also important, since it acts on the calcium and potassium channels in the cell membrane, affecting coordinated cellular functioning and giving rise to neuropsychological disorders [13,15]. Likewise, cadmium (Cd) is classified within the first group of carcinogens by the International Agency for Research on Cancer (IARC) as a highly toxic metal [16,17]. It also causes decreased bone density and kidney damage [18]. Finally, mercury is a toxic metallic element that affects human health, wildlife, aquatic ecosystems (severe and persistent toxicity has been documented from the contaminated fish consumption from fresh and marine waters [4]) and, in general, soils, water and air [19–24].

Resorcin[4]arenes (Figure 1) and their functionalized derivatives have been widely used for complexation studies. Both the selectivity of these ligands towards a given guest [25–28] and the stability of the complexes formed are determined by factors such as geometric complementarity, the types of interactions [25,29] and the nature of the substituents in the macrocycle [30–33]. The stability of the complex is determined by the magnitude of the complex formation constant,  $\beta_f$  [34,35]. Information about host-guest interactions can be derived from its value. The macrocycles evaluated were tetrasodium 5,11,17,23-tetrakisulfonatemethylen 2,8,14,20-tetra(butyl)resorcin[4]arene (Na<sub>4</sub>BRA) and tetrasodium 5,11,17,23-tetrakisulfonatemethylen-2,8,14,20-tetra(2-(methylthio)ethyl)resorcin[4]arene (Na<sub>4</sub>SRA), whose structures are shown in Figure 2.

There are several simple experimental techniques that can be used to determine the stoichiometry and stability constants of complex species. Among the most widely used are conductometry, sonometry, ion-selective potentiometry (ISE), acid-base potentiometry, nuclear magnetic resonance (NMR), UV-VIS spectroscopy and isothermal titration calorimetry (ITC). In the present case, the techniques used to study the complexation of Na<sub>4</sub>BRA and Na<sub>4</sub>SRA with the heavy metals of interest are shown in Table 1.

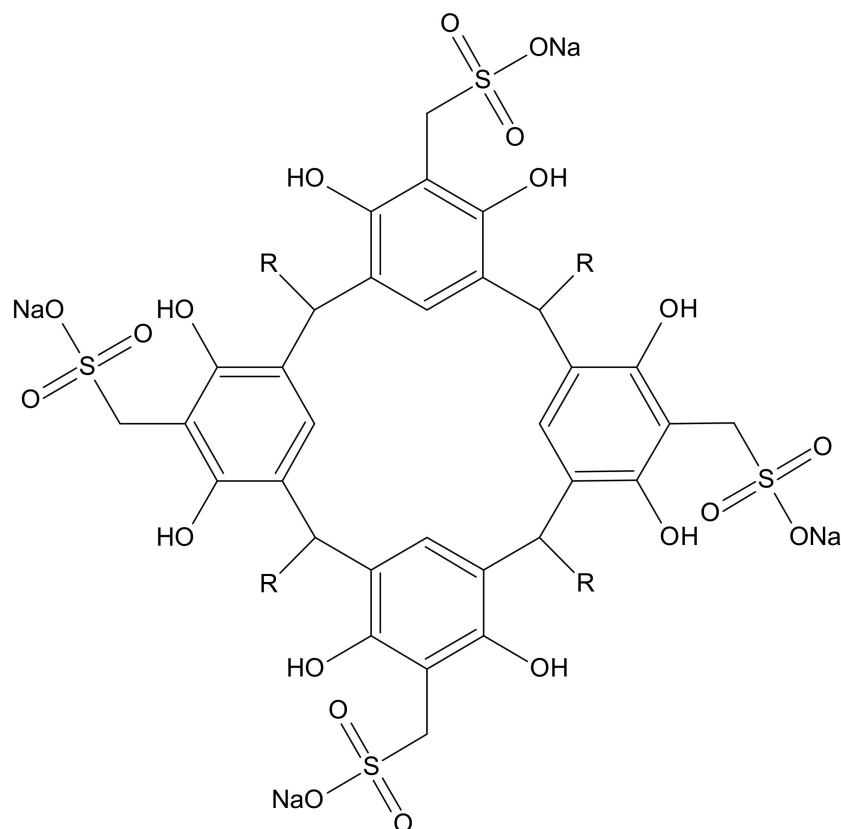


**Figure 1.** Resorcin[4]arene sulfonate structure (Na<sub>4</sub>RA).

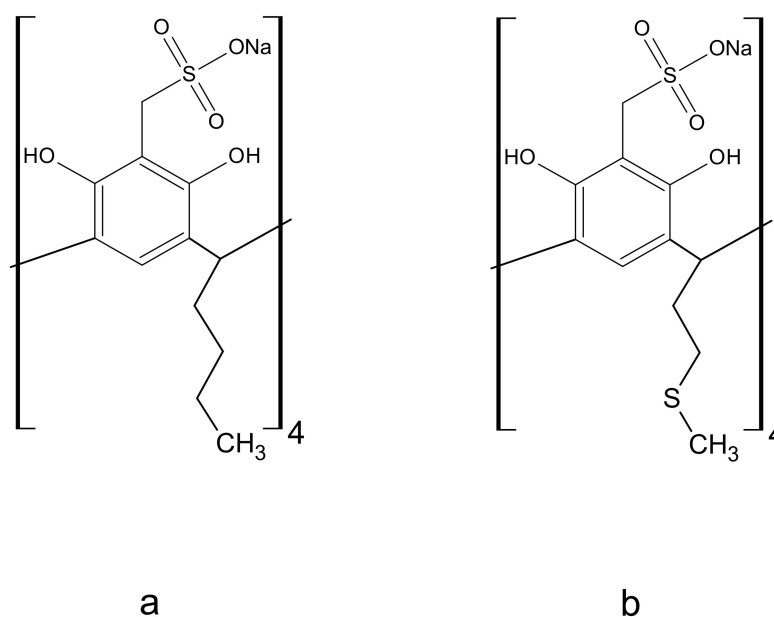


**Figure 2.** Resorcin[4]arenes sulfonated, whose complexing properties with  $\text{Cu}^{2+}$ ,  $\text{Pb}^{2+}$ ,  $\text{Cd}^{2+}$  and  $\text{Hg}^{2+}$  were evaluated. (a) Tetrasodium 5,11,17,23-tetrakisulfonate methylen-2,8,14,20-tetra(butyl)resorcin[4]arene ( $\text{Na}_4\text{BRA}$ ). (b) Tetrasodium 5,11,17,23-tetrakisulfonatemethylen-2,8,14,20-tetra(2-(methylthio) ethyl)resorcin[4]arene ( $\text{Na}_4\text{SRA}$ ).

**Table 1.** Techniques used to study the complexation of heavy metals with  $\text{Na}_4\text{BRA}$  and  $\text{Na}_4\text{SRA}$ .

| Host                    | $\text{Cu}^{2+}$                                   | $\text{Pb}^{2+}$                   | $\text{Cd}^{2+}$ | $\text{Hg}^{2+}$                   |
|-------------------------|--|------------------------------------|------------------|------------------------------------|
| $\text{Na}_4\text{BRA}$ | Conductometry<br>Ion-selective potentiometry (ISE) | Conductometry<br>Atomic absorption | ·Conductometry   | Conductometry                      |
| $\text{Na}_4\text{SRA}$ | Conductometry                                      | Conductometry                      | ·Conductometry   | Conductometry<br>Atomic absorption |

The process of recognition and evaluation of the selectivity of the resorcin[4]arenes was carried out in water by using the conductivity technique, and the positive findings were confirmed by other techniques such as ion-selective potentiometry (ISE) and atomic absorption. The results are discussed in terms of the structure and three-dimensional arrangement of each macrocycle.

## 2. Materials and Methods

### 2.1. Materials

$\text{Na}_4\text{BRA}$  and  $\text{Na}_4\text{SRA}$  were synthesized, purified and characterized according to the procedures described by Sanabria et al. [36]. Heavy metal perchlorates used as guests were used as supplied without further purification; they were stored in amber flasks and dried *in vacuo* over activated silica gel; their purities are shown in Table 2. Water used to prepare the solutions for the conductivity complexation, potentiometry and atomic absorption tests was obtained from a Milli-Q purifier, and it was degassed before use; its conductivity was always  $<0.1 \mu\text{S}\cdot\text{cm}^{-1}$ . The solutions were prepared by weight and corrected to *in vacuo* using an OHAUS Analytical Plus balance (AP250D) (Ohaus Corporation, Florham Park, NJ, USA) that has an accuracy of  $1 \times 10^{-5}$  g in the range of 80 g and  $1 \times 10^{-4}$  g in the range from 80 g up to 250 g.

**Table 2.** Heavy metal salts used for the complexation study with Na<sub>4</sub>BRA and Na<sub>4</sub>SRA.

| Substance   | Source     | Purity   |
|---|------------|----------|
| Cu(ClO <sub>4</sub> ) <sub>2</sub> ·6H <sub>2</sub> O | Alfa Aesar | >98%     |
| Pb(ClO <sub>4</sub> ) <sub>2</sub> ·3H <sub>2</sub> O | Alfa Aesar | 97% min. |
| Cd(ClO <sub>4</sub> ) <sub>2</sub> ·6H <sub>2</sub> O | Alfa Aesar | >99%     |
| Hg(ClO <sub>4</sub> ) <sub>2</sub> ·3H <sub>2</sub> O | Alfa Aesar | >99%     |

## 2.2. Equipments and Experimental Techniques

### 2.2.1. Conductometry

Conductometry has been commonly used in complexation studies between macrocycle ligands and different types of ions [37,38]. The stability constants found by conductometry have been reported in the literature for various macrocycles, among which are:  $\alpha$  and  $\beta$ -cyclodextrins [39,40], alkylcalix[4]arenes [41] and crown ethers [41,42].

Conductivity measurements were carried out using a VEB hydromat Bannewitz LM 3000 cell (Bannewitz, Germany) with a cell constant of  $K_{\text{cell}} = 1.04 \text{ cm}^{-1}$ . It is made of borosilicate glass and provided with two platinum electrodes. The cell was placed inside a 120 mL jacketed glass vessel and kept at a constant temperature of  $(298.15 \pm 0.01) \text{ K}$ , by circulating water through the outer jacket, using a Julabo LC6 temperature controller (Julabo Labortechnik, Seelbach, Germany). The cell was carefully washed, purged with deionized water and dried at  $105 \text{ }^\circ\text{C}$  before use. To avoid the presence of CO<sub>2</sub>, nitrogen gas was passed through the cell before performing each determination. Resistance measurements were carried out with a Stanford SR720 (US) LCR meter (Stanford Research Systems, Sunnyvale, CA, USA) whose accuracy is 0.05%. A voltage of 1.0 V, at a frequency of 1 kHz, was used for all measurements. In a typical complex formation experiment, 40 mL of approximately  $1 \times 10^{-3} \text{ M}$  Na<sub>4</sub>RA aqueous solution were placed into a titration cell and thermostated at 298.15 K. Once the solution reached thermal equilibrium, the resistance of the solution was measured with the LCR meter, and then it was titrated with a ten-times more concentrated guest solution (approximately  $1 \times 10^{-2} \text{ M}$ ). This titration solution was added in 0.1 mL portions, using a metrohm (Metrohm Ltd., Herisau, Switzerland) digital burette, until a ratio of 5/1 (guest/host) was reached. After each addition, the solution was stirred for 20 s, allowed to stand for another 20 s, and its resistance was recorded. The above procedure was carried out with all the proposed metals. A blank was run for each experiment using water instead of the Na<sub>4</sub>RA solution [25].

### 2.2.2. Ion-Selective Potentiometry (ISE)

Ion-selective electrodes have been successfully used for the determination of complex stability constants [43]. The general procedure consists of carrying out titration, at a constant ionic strength of a solution of the guest with the host, while measuring the potential. The formation of 1:1 complexes of Na<sub>4</sub>RA with a M<sup>2+</sup> cation can be represented by the equilibrium:



whose stability constant, at pH 7, can be obtained using the hyperquad software (Wiley Organics, Inc., Coshocton, OH, USA) [44].

Potentiometric titration was carried out only with the Na<sub>4</sub>BRA-Cu<sup>2+</sup> system. For this, a Cu<sup>2+</sup> ion-selective electrode (Cu-ISE, Orion model 94-29, (ThermoFisher Scientific, Waltham, MA, USA) filled with 0.1 N potassium nitrate solution) was used. As in the case of conductivity titrations, it was carried out in a 120 mL jacketed glass cell, and the temperature was kept constant at 298.15 K by circulating water, through the said jacket, from a bath equipped with a Julabo LC6 thermostat (Julabo Labortechnik, Seelbach, Germany), that ensures a temperature control of  $\pm 0.001$  degrees. The calibration curve was prepared with solutions of 0, 1, 10, 100, 300, 600, 800 and 1000 ppm and the ionic strength was controlled with 0.01M NaClO<sub>4</sub>. For the sample analysis, 20 mL of  $2.9 \times 10^{-4} \text{ M}$  Cu(ClO<sub>4</sub>)<sub>2</sub> solution were placed inside the titration vessel thermostated at 298.15 K; once equilibrium

was reached, the sample was titrated using a Metrohm burette (Metrohm Ltd., Herisau, Switzerland) with an  $8.3 \times 10^{-4}$  M  $\text{Na}_4\text{BRA}$  solution [25]. The sample voltage was recorded after each addition, and subsequently, the value obtained was interpolated in the calibration curve to determine the  $\text{Cu}^{2+}$  concentration.

### 2.2.3. Atomic Absorption

This is not a technique used to find the formation constant of a complex, but it allows to determine in a simple, fast and selective way the percentage of metal present in a complex and thus verify the stoichiometric ratio determined by other techniques.

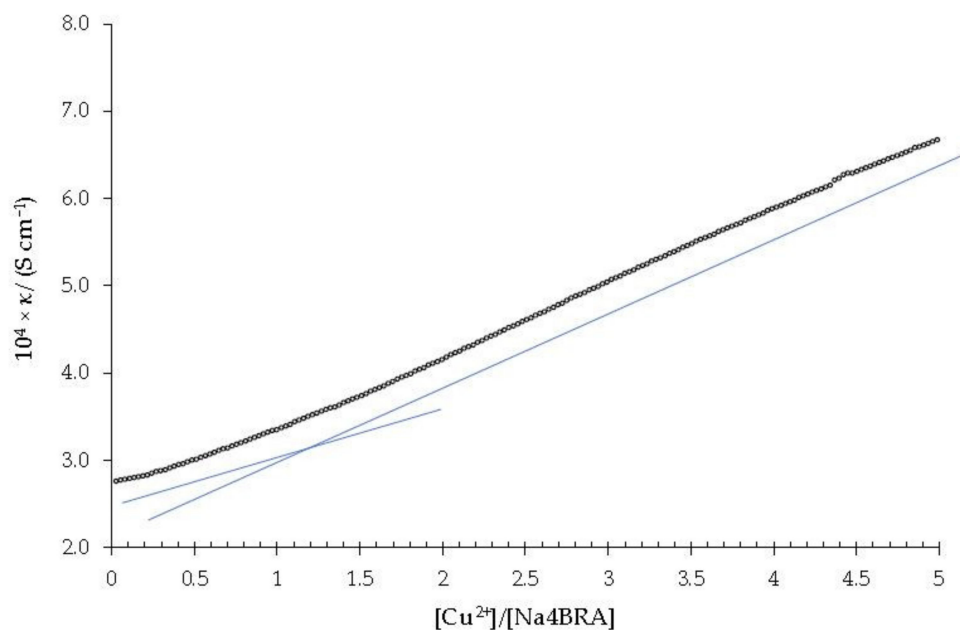
The conductometric titration of both  $\text{Na}_4\text{BRA}$  with  $\text{Pb}(\text{ClO}_4)_2$  and  $\text{Na}_4\text{SRA}$  with  $\text{Hg}(\text{ClO}_4)_2$  produced precipitates three hours after the end of the titration. In both cases, the precipitate was filtered, washed with plenty of water, dried and analyzed by atomic absorption. For this analysis, a Perkin Elmer Analyst 300 spectrophotometer (Perkin Elmer Ltd., Wembley, UK) with an air-acetylene flame in a 10:2 ratio, 0.70 slot, and AAwinlab software was used. The corresponding calibration curve for each metal ion was created by dilution from a concentrated solution of 1000 ppm of  $\text{Me}(\text{NO}_3)_2$ ; the final concentrations obtained were: 1, 4, 8, 12, 16 and 20 ppm of  $\text{Me}^{2+}$ . The complex with either Pb or Hg was digested with nitric acid and afterwards analyzed. The absorbance of the sample was determined in triplicate and the concentration was obtained by interpolation in the corresponding calibration curve [25].

## 3. Results and Discussion

The complexation measurements were carried out in water at 298.15 K and  $\text{pH} = 7$ . According to the species distribution diagram, under these conditions, the predominant species is  $\text{H}_8\text{L}^{4-}$  for both  $\text{Na}_4\text{BRA}$  and  $\text{Na}_4\text{SRA}$  [25].

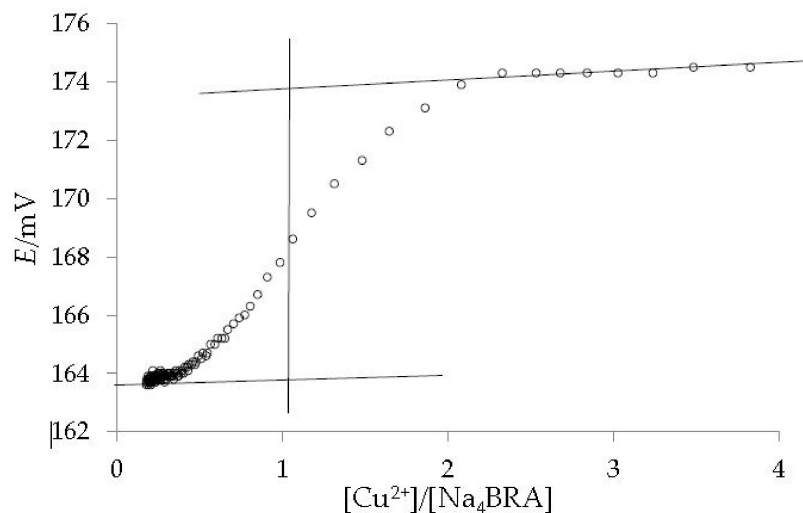
### 3.1. Complexation of $\text{Na}_4\text{BRA}$ with $\text{Cu}^{2+}$

Figure 3 shows the dependence of the specific conductivity against the  $[\text{Cu}^{2+}]/[\text{Na}_4\text{BRA}]$  ratio.



**Figure 3.** Specific conductivity *versus* the  $[\text{Cu}^{2+}]/[\text{Na}_4\text{BRA}]$  ratio. The solid blue lines (which are represented displaced parallel for better visualization) are shown as a visual aid to indicate the cut-off point that relates to the change in the slope of the specific conductivity with respect to the stoichiometry of the complex.

As it can be ascertained, a slight change in slope is observed for a  $[\text{Cu}^{2+}]/[\text{Na}_4\text{BRA}]$  ratio of approximately 1.2, which could suggest the presence of a complex of 1:1 stoichiometry. Both the presence of the complex and its stoichiometry were confirmed by potentiometric titration with a copper selective electrode (Cu-ISE). The dependence between the potential and the  $[\text{Cu}^{2+}]/[\text{Na}_4\text{BRA}]$  ratio is shown in Figure 4.



**Figure 4.** Potentiometric titration of  $\text{Cu}^{2+}$  with  $\text{Na}_4\text{BRA}$ , using a copper selective electrode (Cu-ISE). The lines are shown as a visual aid to identify the 1:1 stoichiometry of the complex.

A value of  $\text{Log } \beta_f = 5.38$ , at 0.01 M ionic strength was determined for the stability constant of the  $[\text{BRA-Cu}]^{2-}$  complex using the Hyperquad software [44,45]. In this sense, higher values are reported in the literature for the stability constants of complexes formed by various metals with p-sulfonatocalixarenes [46].

### 3.2. Complexation of $\text{Na}_4\text{BRA}$ with $\text{Pb}^{2+}$

Figure 5 shows the dependence of the specific conductivity against the  $[\text{Pb}^{2+}]/[\text{Na}_4\text{BRA}]$  ratio.

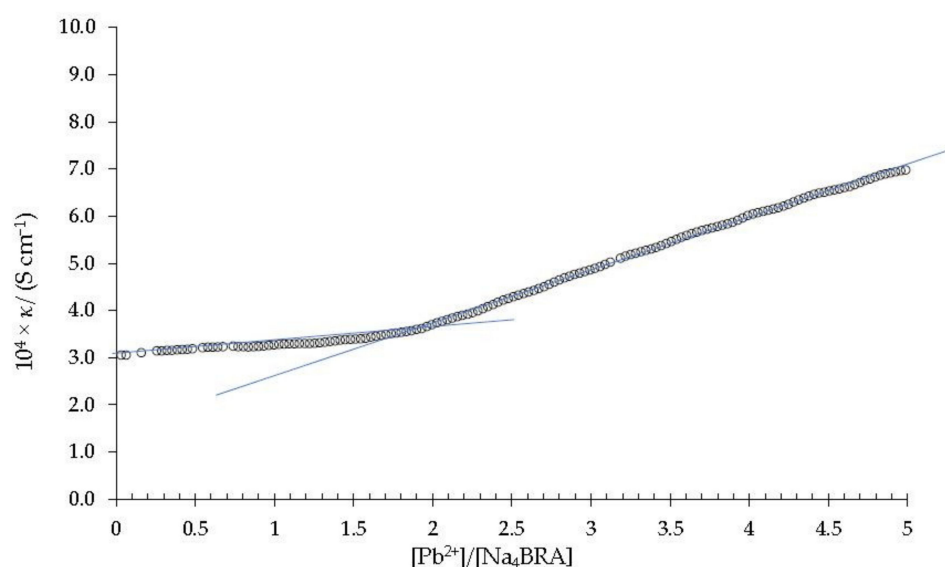


**Figure 5.** Specific conductivity *versus* the  $[\text{Pb}^{2+}]/[\text{Na}_4\text{BRA}]$  ratio. The solid blue lines are shown as a visual aid to indicate the cut-off point that relates the change in slope of the specific conductivity with respect to the stoichiometry of the complex.

As it can be seen, an abrupt change in slope appears at a value of 1.9 in the  $[\text{Pb}^{2+}]/[\text{Na}_4\text{BRA}]$  ratio, approximately. According to Ashram [47] and Jalali and cols. the abrupt changes in the slopes of these specific conductivity plots are related to the formation of stable complexes [41]. Therefore, this suggests the presence of a strong and stable complex between  $\text{Na}_4\text{BRA}$  and  $\text{Pb}^{2+}$ ,  $\text{BRA-Pb}$ , of 1:2 stoichiometry. On the other hand, since this complex precipitates approximately three hours after titration as a fine pink powder [25], it was isolated, purified and analyzed by atomic absorption as indicated in the previous section. The lead content determined in the sample was 25%, which corresponds to a 1:2 stoichiometry for the  $\text{BRA-Pb}$  complex. This result agrees perfectly with that obtained by conductometric titration and can be explained as the result of the electrostatic interactions between the four sulfonate groups of  $\text{BRA}^{4-}$  and two  $\text{Pb}^{2+}$  cations.

### 3.3. Complexation of $\text{Na}_4\text{BRA}$ with either $\text{Cd}^{2+}$ or $\text{Hg}^{2+}$

Figure 6 shows the dependence between the specific conductivity and the  $[\text{Hg}^{2+}]/[\text{Na}_4\text{BRA}]$  and  $[\text{Cd}^{2+}]/[\text{Na}_4\text{BRA}]$  ratios.

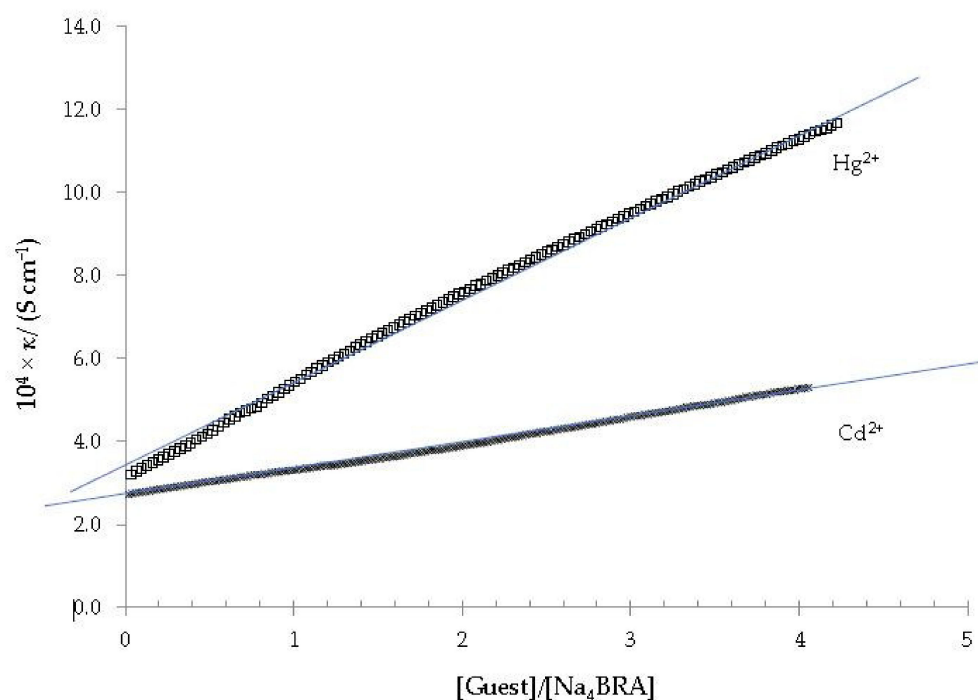


**Figure 6.** Specific conductivity *versus* the  $[\text{Hg}^{2+}]/[\text{Na}_4\text{BRA}]$  and  $[\text{Cd}^{2+}]/[\text{Na}_4\text{BRA}]$  ratios. The solid blue lines are displayed as a visual aid to see that there is no appreciable change in the slope of the plot.

As it can be seen in both cases, the appearance of a change in slope is not observed in these plots, so the formation of  $\text{Cd}^{2+}$  or  $\text{Hg}^{2+}$  complexes with  $\text{Na}_4\text{BRA}$  must be ruled out.

### 3.4. Complexation of $\text{Na}_4\text{SRA}$ with $\text{Hg}^{2+}$

Figure 7 shows the dependence of the specific conductivity with the  $[\text{Hg}^{2+}]/[\text{Na}_4\text{SRA}]$  ratio.

As it can be seen, there is a significant change in the slope of the plot for a ratio  $[\text{Hg}^{2+}]/[\text{Na}_4\text{SRA}]$  equal to 1, which clearly indicates the formation of a stable complex of 1:1 stoichiometry [41,47]. As in the case of  $[\text{BRA-Pb}]$ , this  $[\text{SRA-Hg}]$  complex precipitates approximately three hours after the end of the titration, appearing as a fine pale-yellow powder [25]. This precipitate was isolated, purified and analysed by atomic absorption to confirm its 1:1 stoichiometry.

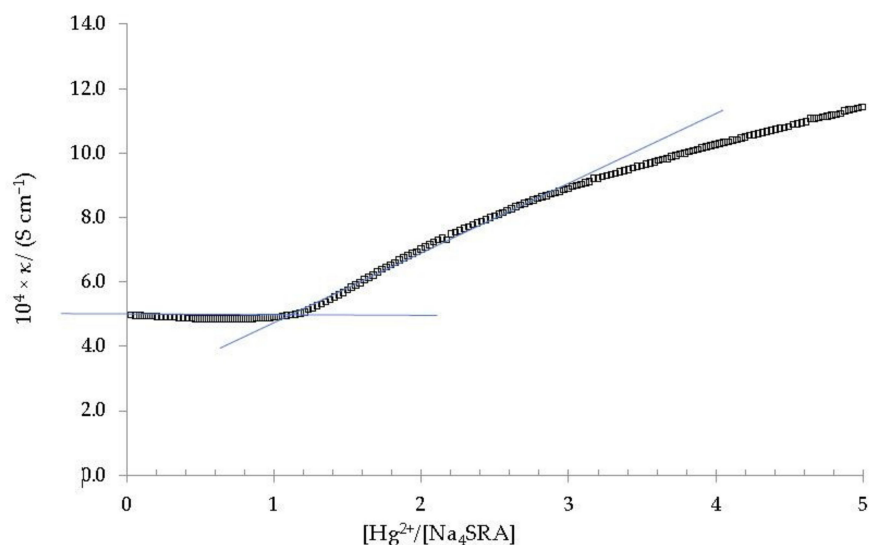


**Figure 7.** Specific conductivity *versus* the  $[\text{Hg}^{2+}]/[\text{Na}_4\text{SRA}]$  ratio. The solid blue lines are shown as a visual aid to indicate the cut-off point that relates the change in slope of the specific conductivity with respect to the stoichiometry of the complex.

The affinity for mercury of sulfur-containing compounds has already been reported by several authors [48,49]. In the case of  $\text{Na}_4\text{SRA}$ , this can be explained as a consequence of the interactions between the  $\text{Hg}^{2+}$  ions and the sulfur donor atoms present at the lower rim of the  $\text{Na}_4\text{SRA}$ .

### 3.5. Complexation of $\text{Na}_4\text{SRA}$ with either $\text{Cu}^{2+}$ , $\text{Pb}^{2+}$ , or $\text{Cd}^{2+}$

Figure 8 shows the dependence of specific conductivity against the  $[\text{guest}]/[\text{Na}_4\text{SRA}]$  ratio.

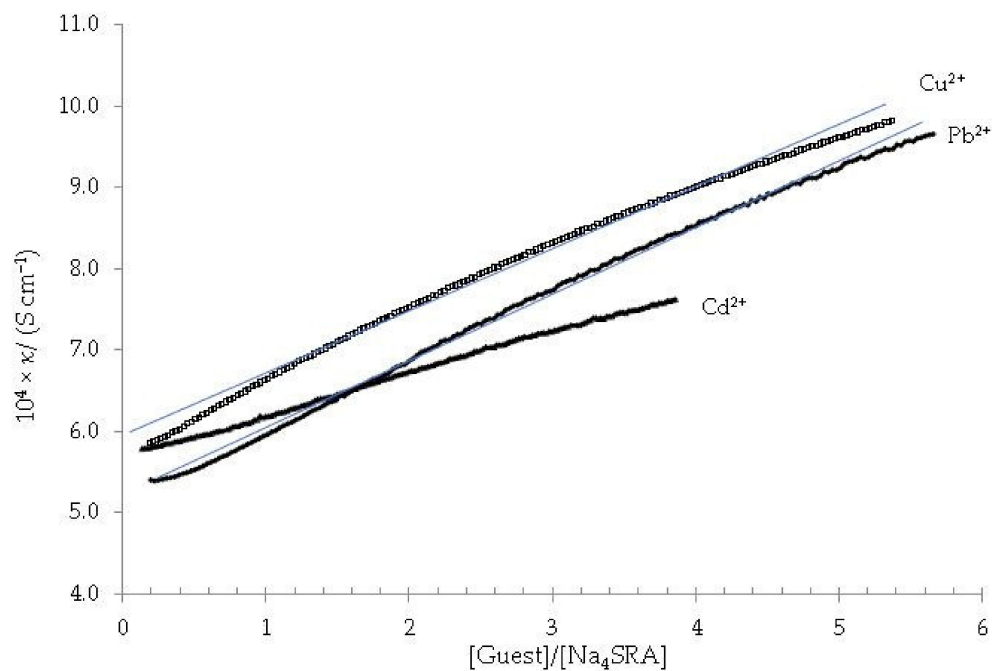


**Figure 8.** Specific conductivity *versus* the  $[\text{guest}]/[\text{Na}_4\text{SRA}]$  ratio; being the guest ( $\Delta$ )  $\text{Pb}^{2+}$ , ( $\diamond$ )  $\text{Cd}^{2+}$ , ( $\bullet$ )  $\text{Cu}^{2+}$ . The solid blue lines are displayed as a visual aid to see that there is no appreciable change in the slope of the plots.

As it is ascertained, in no case a change in the slope is observed, so it must be deduced that none of the  $\text{Na}_4\text{SRA-Pb}^{2+}$ ,  $\text{Na}_4\text{SRA-Cu}^{2+}$  and  $\text{Na}_4\text{SRA-Cd}^{2+}$  systems show complexation.

Table 3 summarizes what has been seen so far, indicating which guest metals form complexes with the hosts  $\text{Na}_4\text{BRA}$  and  $\text{Na}_4\text{SRA}$ .

**Table 3.** Stoichiometry of the complexes formed with the hosts  $\text{Na}_4\text{BRA}$  and  $\text{Na}_4\text{SRA}$ .

| Host/Guest              | $\text{Cu}^{2+}$ | $\text{Pb}^{2+}$ | $\text{Cd}^{2+}$ | $\text{Hg}^{2+}$ |
|-------------------------|------------------|------------------|------------------|------------------|
| $\text{Na}_4\text{BRA}$ | 1:1              | 1:2              | -                | -                |
| $\text{Na}_4\text{SRA}$ | -                | -                | -                | 1:1              |

According to the above table,  $\text{Na}_4\text{SRA}$  selectively complexes  $\text{Hg}^{2+}$ , while  $\text{Na}_4\text{BRA}$  complexes  $\text{Cu}^{2+}$  and  $\text{Pb}^{2+}$ . The fact that  $\text{Na}_4\text{BRA}$  complexes two guests and  $\text{Na}_4\text{SRA}$  only one can be explained on the basis of the greater conformational stability of  $\text{Na}_4\text{BRA}$  compared to  $\text{Na}_4\text{SRA}$ , caused by Van der Waals-type interactions between the lower edge chains of  $\text{Na}_4\text{BRA}$ , whereas in the case of  $\text{Na}_4\text{SRA}$ , conformational mobility can prevent the entry or facilitate the exit of the guest through the upper edge of the host. Additionally, due to the presence of sulfur at the lower edge of  $\text{Na}_4\text{SRA}$ , this can form bonds with hydrogen from water, which could prevent the inclusion of some guests within the host. In the case of the  $[\text{SRA-Hg}]^{2+}$  complex, this situation does not occur since mercury can interact with the sulfur donor atoms of  $\text{Na}_4\text{SRA}$ .

#### 4. Conclusions

The complexing properties of  $\text{Na}_4\text{BRA}$  and  $\text{Na}_4\text{SRA}$  were studied by conductometry, and the positive results were confirmed by other techniques such as ion-selective potentiometry (ISE) and atomic absorption. The results indicate that  $\text{Na}_4\text{BRA}$  is able to complex  $\text{Cu}^{2+}$  in a 1:1 ratio and  $\text{Pb}^{2+}$  in a 1:2 ratio. Regarding the complex formed by  $\text{Na}_4\text{SRA}$  with  $\text{Hg}^{2+}$ , the ratio found was 1:1. In this latter case, the results suggest that the interaction between the  $\text{Hg}^{2+}$  ions and the sulfur atoms present at the lower edge of the  $\text{SRA}^{4-}$  is greater than that established between these latter atoms and the hydrogens of the solvent (an interaction that would prevent the entry of the guest into the cavity of the  $\text{SRA}^{4-}$ ), which favors the entry of  $\text{Hg}^{2+}$  and means that the  $\text{Na}_4\text{SRA}$  are selective for these ions.

**Author Contributions:** Conceptualization, E.S., M.A.E. and E.F.V.; Methodology, E.S., M.A.E. and E.F.V.; Validation, E.S. and M.A.E.; Formal analysis, E.S.; Investigation, E.S.; Resources, E.S. and E.F.V.; Writing—original draft preparation, E.S.; Writing—review and editing, M.A.E. and E.F.V.; Supervision, M.A.E. and E.F.V.; Project administration, E.S., M.A.E. and E.F.V.; Funding acquisition, E.S. All authors have read and agreed to the published version of the manuscript.

**Funding:** This research received no external funding.

**Institutional Review Board Statement:** Not applicable.

**Informed Consent Statement:** Not applicable.

**Data Availability Statement:** Not applicable.

**Conflicts of Interest:** The authors declare no conflict of interest.

## References

1. Rahman, Z.; Jagadheeswari; Mohan, A.; Priya, S.; Tharini; Selvendran. Electrokinetic remediation: An innovation for heavy metal contamination in the soil environment. *Mater. Today Proc.* **2021**, *37*, 2730–2734. [[CrossRef](#)]
2. Gujre, N.; Mitra, S.; Soni, A.; Agnihotri, R.; Rangan, L.; Rene, E.R.; Sharma, M.P. Speciation, contamination, ecological and human health risks assessment of heavy metals in soils dumped with municipal solid wastes. *Chemosphere* **2021**, *262*, 128013. [[CrossRef](#)] [[PubMed](#)]
3. Khan, S.; Naushad, M.; Lima, E.C.; Zhang, S.; Shaheen, S.M.; Rinklebe, J. Global soil pollution by toxic elements: Current status and future perspectives on the risk assessment and remediation strategies—A review. *J. Hazard. Mater.* **2021**, *417*, 126039. [[CrossRef](#)] [[PubMed](#)]
4. Robinson, J.; Shroff, J. Observations on the levels of total mercury (Hg) and selenium (Se) in species common to the artisanal fisheries of Seychelles. *NeuroToxicology* **2020**, *81*, 277–281. [[CrossRef](#)]
5. Liu, P.; Yang, Y.; Li, M. Responses of soil and earthworm gut bacterial communities to heavy metal contamination. *Environ. Pollut.* **2020**, *265*, 114921. [[CrossRef](#)]
6. Baruah, S.G.; Ahmed, I.; Das, B.; Ingtipi, B.; Boruah, H.; Gupta, S.K.; Nema, A.K.; Chabukdhara, M. Heavy metal(loid)s contamination and health risk assessment of soil-rice system in rural and peri-urban areas of lower brahmaputra valley, northeast India. *Chemosphere* **2021**, *266*, 129150. [[CrossRef](#)]
7. Ma, J.; Chen, Y.; Antoniadis, V.; Wang, K.; Huang, Y.; Tian, H. Assessment of heavy metal(loid)s contamination risk and grain nutritional quality in organic waste-amended soil. *J. Hazard. Mater.* **2020**, *399*, 123095. [[CrossRef](#)]
8. Okereafor, U.; Makhatha, M.; Mekuto, L.; Uche-Okereafor, N.; Sebola, T.; Mavumengwana, V. Toxic Metal Implications on Agricultural Soils, Plants, Animals, Aquatic life and Human Health. *Int. J. Environ. Res. Public Health* **2020**, *17*, 2204. [[CrossRef](#)]
9. Cruzado-Tafur, E.; Torró, L.; Bierla, K.; Szpunar, J.; Tauler, E. Heavy metal contents in soils and native flora inventory at mining environmental liabilities in the Peruvian Andes. *J. South Am. Earth Sci.* **2021**, *106*, 103107. [[CrossRef](#)]
10. Peixoto, R.R.A.; Jadán-Piedra, C. Cadmium pollution of water, soil, and food: A review of the current conditions and future research considerations in Latin America. *Environ. Rev.* **2021**, *30*, 110–127. [[CrossRef](#)]
11. Moon, M.K.; Lee, I.; Lee, A.; Park, H.; Kim, M.J.; Kim, S.; Cho, Y.H.; Hong, S.; Yoo, J.; Cheon, G.J.; et al. Lead, mercury, and cadmium exposures are associated with obesity but not with diabetes mellitus: Korean National Environmental Health Survey (KoNEHS) 2015–2017. *Environ. Res.* **2022**, *204*, 111888. [[CrossRef](#)]
12. Islam, S.; Proshad, R.; Haque, M.A.; Hoque, F.; Hossin, S.; Sarker, N.I. Assessment of heavy metals in foods around the industrial areas: Health hazard inference in Bangladesh. *Geocarto. Int.* **2020**, *35*, 280–295. [[CrossRef](#)]
13. Pan, S.; Lin, L.; Zeng, F.; Zhang, J.; Dong, G.; Yang, B.; Jing, Y.; Chen, S.; Zhang, G.; Yu, Z.; et al. Effects of lead, cadmium, arsenic, and mercury co-exposure on children's intelligence quotient in an industrialized area of southern China. *Environ. Pollut.* **2018**, *235*, 47–54. [[CrossRef](#)]
14. Osredkar, J.; Sustar, N. Copper and Zinc, Biological Role and Significance of Copper/Zinc Imbalance. *J. Clin. Toxicol.* **2011**, *s3*, 0495. [[CrossRef](#)]
15. Garza, A.; Vega, R.; Soto, E. Cellular mechanisms of lead neurotoxicity. *Med. Sci. Monit.* **2006**, *12*, RA57–RA65.
16. Glicklich, D.; Frishman, W.H. The Case for Cadmium and Lead Heavy Metal Screening. *Am. J. Med. Sci.* **2021**, *362*, 344–354. [[CrossRef](#)]
17. Es-Sahbany, H.; El Hachimi, M.; Hsissou, R.; Belfaquir, M.; Nkhili, S.; Loutfi, M.; Elyoubi, M. Adsorption of heavy metal (Cadmium) in synthetic wastewater by the natural clay as a potential adsorbent (Tangier-Tetouan-Al Hoceima–Morocco region). *Mater. Today: Proc.* **2021**, *45*, 7299–7305. [[CrossRef](#)]
18. Qing, Y.; Yang, J.; Chen, Y.; Shi, C.; Zhang, Q.; Ning, Z.; Yu, Y.; Li, Y. Urinary cadmium in relation to bone damage: Cadmium exposure threshold dose and health-based guidance value estimation. *Ecotoxicol. Environ. Saf.* **2021**, *226*, 112824. [[CrossRef](#)]
19. Wang, B.; Chen, M.; Ding, L.; Zhao, Y.; Man, Y.; Feng, L.; Li, P.; Zhang, L.; Feng, X. Fish, rice, and human hair mercury concentrations and health risks in typical Hg-contaminated areas and fish-rich areas, China. *Environ. Int.* **2021**, *154*, 106561. [[CrossRef](#)]
20. Garcia-Ordiales, E.; Roqueñí, N.; Loredo, J. Mercury bioaccumulation by *Juncus maritimus* grown in a Hg contaminated salt marsh (northern Spain). *Mar. Chem.* **2020**, *226*, 103859. [[CrossRef](#)]
21. Zheng, W.; Chandan, P.; Steffen, A.; Stuppel, G.; De Vera, J.; Mitchell, C.P.; Wania, F.; Bergquist, B.A. Mercury stable isotopes reveal the sources and transformations of atmospheric Hg in the high Arctic. *Appl. Geochem.* **2021**, *131*, 105002. [[CrossRef](#)]
22. Liu, Q.; Xu, X.; Zeng, J.; Huang, W.; Xu, X.; Shou, L.; Chen, Q. Development of marine water quality criteria for inorganic mercury in China based on the retrievable toxicity data and a comparison with relevant criteria or guidelines. *Ecotoxicology* **2019**, *28*, 412–421. [[CrossRef](#)]
23. Wang, L.; Hou, D.; Cao, Y.; Ok, Y.S.; Tack, F.M.G.; Rinklebe, J.; O'Connor, D. Remediation of mercury contaminated soil, water, and air: A review of emerging materials and innovative technologies. *Environ. Inter.* **2020**, *134*, 105281. [[CrossRef](#)]
24. Cheng, Y.; Zhang, R.; Li, T.; Zhang, F.; Russell, J.; Guan, M.; Han, Q.; Zhou, Y.; Xiao, X.; Wang, X. Spatial distributions and sources of heavy metals in sediments of the Changjiang Estuary and its adjacent coastal areas based on mercury, lead and strontium isotopic compositions. *CATENA* **2019**, *174*, 154–163. [[CrossRef](#)]

25. Sanabria, E. Physicochemical Study of Resorcin[4]arenes Sulfonated in Aqueous Solution and Its Complexity with Ions of Interest. Ph.D. Thesis, University of Los Andes, Bogotá, Colombia, 2016. Available online: <https://ebuah.uah.es/dspace/bitstream/handle/10017/26597/Tesis%20Edilma%20Sanabria%20Espa%C3%B1ol.pdf?sequence=1&isAllowed=y> (accessed on 30 June 2022).
26. Jain, V.K.; Kanaiya, P.H. Chemistry of calix[4]resorcinarenes. *Russ. Chem. Rev.* **2011**, *80*, 75–102. [[CrossRef](#)]
27. Kazakova, E.K.; Ziganshina, A.; Muslinkina, L.A.; Morozova, J.; Makarova, N.A.; Mustafina, A.R.; Habicher, W.D. The Complexation Properties of the Water-Soluble Tetrasulfonatomethylcalix[4]resorcinarene toward  $\alpha$ -Aminoacids. *J. Incl. Phenom. Macrocycl. Chem.* **2002**, *43*, 65–69. [[CrossRef](#)]
28. Skripacheva, V.V.; Kazakova, E.K.; Markarova, N.A.; Kataev, V.E.; Ermolaeva, L.V.; Habicher, W.D. A Water soluble Sulfonatomethylated Calix[4]resorcinarene as Artificial Receptor of Metal Complexes. *J. Incl. Phenom. Macrocycl. Chem.* **2002**, *42*, 77–81. [[CrossRef](#)]
29. Wang, J.; Liu, D.; Guo, X.; Yan, C. Ammonium and imidazolium-based amphiphilic tetramethoxy resorcinarenes: Adsorption, micellization, and protein binding. *J. Mol. Liq.* **2020**, *313*, 113587. [[CrossRef](#)]
30. Shalaeva, Y.; Morozova, J.E.; Gubaidullin, A.; Saifina, A.; Shumatbaeva, A.; Nizameev, I.; Kadirov, M.; Ovsyannikov, A.; Antipin, I. Photocatalytic properties of supramolecular nanoassociates based on gold and platinum nanoparticles, capped by amphiphilic calix[4]resorcinarenes, towards organic dyes. *Colloids Surf. A Physicochem. Eng. Asp.* **2020**, *596*, 124700. [[CrossRef](#)]
31. Sanabria, E.; Estesio, M.; Vargas, E.; Maldonado, M. Experimental comparative study of solvent effects on the structure of two sulfonated resorcinarenes. *J. Mol. Liq.* **2018**, *254*, 391–397. [[CrossRef](#)]
32. Español, E.S.; Villamil, M.M.; Estesio, M.A.; Vargas, E.F. Volumetric and acoustic properties of two sodium sulfonateresorcin[4]arenes in water and dimethylsulfoxide. *J. Mol. Liq.* **2018**, *249*, 868–876. [[CrossRef](#)]
33. Mironova, D.A.; Muslinkina, L.A.; Morozova, J.E.; Shalaeva, Y.V.; Kazakova, E.K.; Kadyrov, M.T.; Nizameev, I.R.; Konovalov, A.I. Complexes of tetramethylsulfonatocalix[4]resorcinarene aggregates with methyl orange: Interactions with guests and driving force of color response. *Colloids Surf. A Physicochem. Eng. Asp.* **2015**, *468*, 339–345. [[CrossRef](#)]
34. Da Silva, E.; Rousseau, C.F.; Zanella-Cleon, I.; Becchi, M.; Coleman, A.W. Mass Spectrometric Determination of Association Constants of Bovine Serum Albumin (BSA) with para-Sulphonato-Calix[n]arene Derivatives. *J. Incl. Phenom. Macrocycl. Chem.* **2006**, *54*, 53–59. [[CrossRef](#)]
35. Ahmadzadeh, S.; Rezayi, M.; Karimi-Maleh, H.; Alias, Y. Conductometric measurements of complexation study between 4-Isopropylcalix[4]arene and  $\text{Cr}^{3+}$  cation in THF–DMSO binary solvents. *Measurement* **2015**, *70*, 214–224. [[CrossRef](#)]
36. Sanabria, E.; Estesio, M.; Pérez-Redondo, A.; Vargas, E.F.; Maldonado, M. Synthesis and Characterization of Two Sulfonated Resorcinarenes: A New Example of a Linear Array of Sodium Centers and Macrocycles. *Molecules* **2015**, *20*, 9915–9928. [[CrossRef](#)]
37. Amirov, R.R.; Nugaeva, Z.T.; Mustafina, A.R.; Fedorenko, S.V.; Morozov, V.I.; Kazakova, E.K.; Habicher, W.D.; Konovalov, A.I. Aggregation and counter ion binding ability of sulfonatomethylcalix[4]resorcinarenes in aqueous solutions. *Colloids Surf. A Physicochem. Eng. Asp.* **2004**, *240*, 35–43. [[CrossRef](#)]
38. Rounaghi, G.H.; Razavipanah, E. Complexation of 4'-nitrobenzo-15-crown-5 with  $\text{Li}^+$ ,  $\text{Na}^+$ ,  $\text{K}^+$ , and  $\text{NH}_4^+$  cations in acetonitrile-methanol binary solutions. *J. Incl. Phenom. Macrocycl. Chem.* **2008**, *61*, 313–318. [[CrossRef](#)]
39. Ali, M.S.; Rub, M.A.; Khan, F.; Al-Lohedan, H.; Din, K.U.  $\beta$ -Cyclodextrin-promazine hydrochloride interaction: Conductometric and viscometric studies. *J. Saudi Chem. Soc.* **2012**, *19*, 83–87. [[CrossRef](#)]
40. Ali, M.S.; Rub, M.A.; Khan, F.; Al-Lohedan, H.A.; Din, K. Interaction of amphiphilic drug amitriptyline hydrochloride with  $\beta$ -cyclodextrin as studied by conductometry, surface tensiometry and viscometry. *J. Mol. Liq.* **2012**, *167*, 115–118. [[CrossRef](#)]
41. Jalali, F.; Ashrafi, A.; Shamsipur, M. Conductance study of the thermodynamics of complexation of amantadine, rimantadine and aminocyclohexane with some macrocyclic compounds in acetonitrile solution. *J. Incl. Phenom. Macrocycl. Chem.* **2007**, *61*, 77–82. [[CrossRef](#)]
42. Vafi, M.; Rounaghi, G.H.; Chamsaz, M. Study of complex formation process between 4'-nitrobenzo-18-crown-6 and yttrium(III) cation in some binary mixed non-aqueous solvents using the conductometry method. *Arab. J. Chem.* **2017**, *10*, 739–745. [[CrossRef](#)]
43. Granholm, K.; Sokalski, T.; Lewenstam, A.; Ivaska, A. Ion-selective electrodes in potentiometric titrations; a new method for processing and evaluating titration data. *Anal. Chim. Acta* **2015**, *888*, 36–43. [[CrossRef](#)]
44. Gans, P.; Sabatini, A.; Vacca, A. Investigation of equilibria in solution. Determination of equilibrium constants with the HYPERQUAD suite of programs. *Talanta* **1996**, *43*, 1739–1753. [[CrossRef](#)]
45. Alderighi, L.; Gans, P.; Ienco, A.; Peters, D.; Sabatini, A.; Vacca, A. Hyperquad simulation and speciation (HySS): A utility program for the investigation of equilibria involving soluble and partially soluble species. *Coord. Chem. Rev.* **1999**, *184*, 311–318. [[CrossRef](#)]
46. Rathod, N.V.; Joshi, K.; Jadhav, A.S.; Kalyani, V.S.; Kalyani, V.S.; Malkhede, D.D. A novel interaction study of Th (IV) 451 and Zr (IV) with 4-sulfonatocalix[6]arene: Experimental and theoretical investigation. *Polyhedron* **2017**, *137*, 207–216. [[CrossRef](#)]
47. Ashram, M.H. Conductance and Thermodynamic Study of the Complexation of Ethyl p-Tert-butylcalix[4]arene Tetraacetate with Alkali Metal and Silver Ions in Various Solvents. *J. Incl. Phenom. Macrocycl. Chem.* **2002**, *42*, 25–31. [[CrossRef](#)]
48. De Namor, A.F.D.; Abbas, I. Sulfur-Containing Hetero-Calix[4]pyrroles as Mercury(II) Cation-Selective Receptors: Thermodynamic Aspects. *J. Phys. Chem. B* **2007**, *111*, 5803–5810. [[CrossRef](#)]
49. Tracey, M.P.; Koide, K. Development of a Sustainable Enrichment Strategy for Quantification of Mercury Ions in Complex Samples at the Sub-Parts per Billion Level. *Ind. Eng. Chem. Res.* **2014**, *53*, 14565–14570. [[CrossRef](#)]